
Article:
Liu, X., Zhao, J., Qiu, G. et al. (4 more authors) (2022) Biological activities of some natural compounds and their cytotoxicity studies against breast and prostate cancer cell lines and anti-COVID19 studies. Journal of Oleo Science, 71 (4). ess21275. pp. 587-597. ISSN 1345-8957

https://doi.org/10.5650/jos.ess21275

Journal of Oleo Science
Copyright ©2022 by Japan Oil Chemists' Society
doi : 10.5650/jos.ess21275
J. Oleo Sci. **71**, *(4) 587-597 (2022)*

Biological Activities of Some Natural Compounds and Their Cytotoxicity Studies against Breast and Prostate Cancer Cell Lines and Anti-COVID19 Studies

Xin Liu[1], Jiangtao Zhao[2], Guoqiang Qiu[3], Tahani Awad Alahmadi[4], Sulaiman Ali Alharbi[5], Milton Wainwright[6], and Wei Duan[7]*

[1] *Department of Intervention Therapy, Lanzhou University Second Hospital, Lanzhou City, Gansu Province, 730030, CHINA*
[2] *Department of General Surgery, Baoding Fourth Central Hospital, Baoding, Hebei Province, 072350, CHINA*
[3] *Department of Pharmacy, Zhangzhou Hospital Affiliated to Fujian Medical University, 363000, CHINA*
[4] *Department of Pediatrics, College of Medicine and King Khalid University Hospital, King Saud University, Medical City, PO Box-2925, Riyadh - 11461, SAUDI ARABIA*
[5] *Department of Botany and Microbiology, College of Science, King Saud University, PO Box -2455, Riyadh -11451, SAUDI ARABIA*
[6] *Department of Molecular Biology and Biotechnology, University of Sheffield, Sheffield S10 2TN, UK*
[7] *Department of Clinical Laboratory, First Affiliated Hospital, School of Medicine, Shihezi University, Shihezi, Xinjiang, 832008, CHINA*

Abstract: In this study, we investigated the inhibition effects of matairesinol, pregnanolone, hamamelitannin, secoisolariciresinol, and secoisolariciresinol diglicoside compounds on HMG-CoA reductase and urease enzymes. We have obtained results for the HMG-CoA reductase enzyme at the millimolar level, and for the urease enzyme at the micromolar level. Molecular docking calculations were made for their biological activities were compared. In docking calculations, proteins of experimentally used enzymes, activities of SARS-CoV-2 virus against RNA-dependent RNA polymerase (RdRp) protein, and anti-oxidant protein were compared. Then, ADME/T calculations were made to use the molecules as drugs. Cytotoxicity potential of these complexes against human breast and prostate cancers demonstrated that these compounds had good cytotoxic effects. There is growing attention to phenolic molecules and their presumed role in avoiding diverse degenerative diseases, such as cardiovascular and cancer diseases.

Key words: phenolic compounds, cytotoxicity, molecular docking, enzyme inhibition, COVID19

1 Introduction

Phenolic molecules are ubiquitously distributed chemicals recorded in most plant tissues, including vegetables and fruits. They are metabolite factors synthesized through the phenylpropanoid pathways and shikimic acid. These compounds possess bioactive properties and also they are not nutrients, dietary intake provides health-protective impacts, for this reason, postharvest treatments have been utilized to increase or preserve the contents of phenolic compounds in vegetables and fruits[1, 2]. HMG-CoA reductase is the enzyme that controls cholesterol synthesis. HMG-CoA reductase is an endoplasmic reticulum inner membrane protein and the catalytic domain of the enzyme extends towards the cytosol. It is the key enzyme of the mevalonate pathway, and the mevalonate pathway is at the beginning of the synthesis of sterols, isoprenoids and other lipids. The reaction catalyzed by HMG-CoA reductase is the rate-determining reaction in the mevalonate pathway[3, 4]. This enzyme is regulated at the levels of translation, transcription, degradation, and phosphorylation. The HMG-CoA reductase inhibitors are agents that have strong blood cholesterol and lipid-lowering effects and are used for primary and secondary prevention in atherosclerosis. However, studies have shown that its mortality-reducing effects in atherosclerosis cannot be explained solely by its lipid-lowering effects. Therefore, these agents have been shown to have anti-inflammatory, immunomodulatory, as well as platelet functions, and procoagulant activity[5, 6].

Bacteria, fungi, yeasts, and plants synthesize urease to provide the nitrogen source necessary for their growth and development. Urease is also a virulence factor found in various pathogenic bacteria. It is therefore not surprising that it is essential in colonizing a host organism and maintaining bacterial cells in tissues[7, 8]. The activity of the

*Correspondence to: Wei Duan, Department of Clinical Laboratory, First Affiliated Hospital, School of Medicine, Shihezi University, Shihezi, Xinjiang, 832008, CHINA
E-mail: duanwei05081@sina.com
Accepted December 10, 2021 (received for review September 11, 2021)
Journal of Oleo Science ISSN 1345-8957 print / ISSN 1347-3352 online
http://www.jstage.jst.go.jp/browse/jos/ http://mc.manusriptcentral.com/jjocs

enzyme leads to various consequences such as the appearance of stones in the urine, blockage in the catheter, ammonia encephalopathy, pyelonephritis, hepatic coma, and gastritis[9, 10].

The SARS-CoV-2 virus is a single stranded genomic RNA virus surrounded by an envelope[11]. It carries RNA as genetic material, and it is the group of viruses with the largest genome among RNA-carrying viruses. When the SARS-CoV-2 virus enters the human metabolism, it looks for a cell to reproduce. When it finds this cell, it tries to glow inside the cell. It has spike-shaped protrusions around the envelope of the SARS-CoV-2 virus. It clings to the receptor on the cell with these protrusions and tries to enter the cell[12]. Once inside the cell, the SARS-CoV-2 virus tries to replicate itself and eventually, the cell explodes itself to death. The SARS-CoV-2 virus, which multiplies in the cell, spreads to other cells, and the disease continues to spread in human metabolism. This situation is shown in Fig. 1.

It is the SARS-CoV-2 virus, one of the most important epidemic diseases of today. The proteins of this virus should be examined in detail and try to find a good inhibitor. For this, molecular docking studies are of great importance[13]. The results of the molecular docking calculations made are an important guide to experimental processes. In this study, it was tried to compare the inhibitory activities against RNA-dependent RNA polymerase (RdRp) protein of SARS-CoV-2 virus protein (pdb ID: 6YYT)[14] in molecular docking calculations. Apart from that, the experimentally studied enzymes are crystal structure of HMG-CoA reductase protein (pdb ID: 1HWL)[15] and crystal structure of Jack bean urease (from Canavalia ensiformis) (pdb ID: 4H9M). Finally, to compare the anti-oxidant activity, the crystal structure of Human peroxiredoxin 5 protein (HP-5) (pdb ID: 1HD2)[16] was used. The molecules used in this study are hamamelitannin, matairesinol, pregnanolone, secoisolariciresinol, and secoisolariciresinol diglicoside. Thiourea, favipiravir[17], and butylated hydroxyanisole (BHA) were used as standard in calculations.

2 Materials and Methods

2.1 Enzymes studies

HMG-CoA reductase activity conforming to the method explained by group of Takahashi[18]; It was measured spectrophotometrically using the absorbance change of NADPH at 340 nm due to the DL-HMG-CoA + 2NADPH + $2H^+ \rightarrow$ (*R*)-mevalonate + $2NADP^+$ + CoASH reaction. Reagents: 1. HMG-CoA: 0.30 mM 2. NADPH: 3 mM 3. NaN_3: 2 M; 4. phosphate buffer: pH: 7.2; 50 mM: Experiment Conducting Spectrophotometer After zero adjustment against distilled water at 340 nm, phosphate buffer is added to the test tubes separately as blank and sample for each sample[19]. NaN_3, NADPH and sample were added and mixed well and the change in absorbance was followed for 1 min. Then HMG-CoA was added to the cuvette and the change in absorbance was followed for 3 min. The activity of HMG-CoA was calculated using the ε coefficient of NADPH. The results were calculated from the ε value of NADPH (ε: 6.22 × 103 L/mol.cm.) is given as IU/L[20].

2.2 Urease inhibition assay

Mobley's method[21] was used to determine the urease inhibition activity. For the urease enzyme inhibition activity, urea was used as substrate after the extracts were interacted with urease enzyme and the ammonia formed as a result of the reaction was determined spectroscopically. Thiourea was used as a positive control. The solutions required for analysis were prepared as follows; 0.01 M Phosphate buffer (pH = 8.2): The pH is adjusted to 8.2 by mixing 0.01 M NaH_2PO_4 and 0.01 M Na_2HPO_4 buffer solutions in appropriate proportions. Urease enzyme: 1 mg urease enzyme is dissolved in 1 mL of buffer solution[22]. When used by dividing into 50 μL portions, appropriate dilution is made in the range of 2000-3000 μL. Substrate: A 0.1 M urea solution (in pH = 8.2 phosphate buffer) is used as the substrate. Phenol reagent: for 1% phenol reagent; 200 mg of phenol is weighed and dissolved in 10 mL of distilled water and 2% phenol reagent is obtained. With sub-

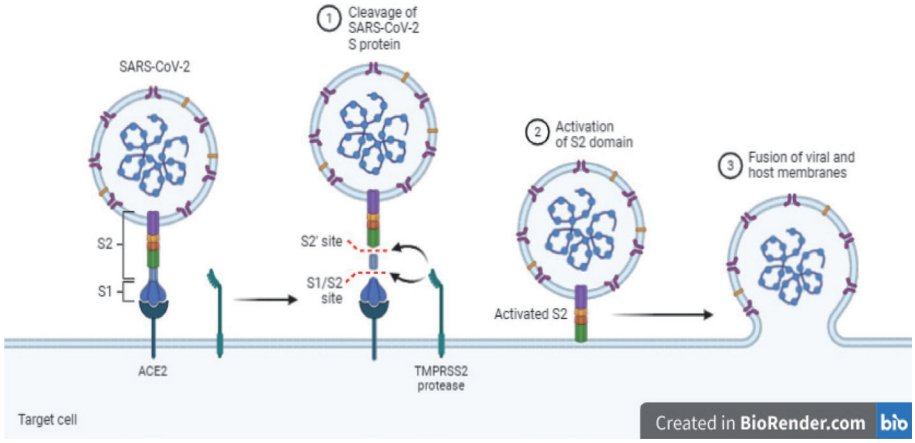

Fig. 1 The method of the SARS-CoV-2 virus to enter the cell.

sequent dilutions, the final concentration will be 1%[23]. For 0.005% sodium nitroprusside; 1 mg of sodium nitroprusside is weighed and dissolved in 10 mL of distilled water and a solution of 0.01% is obtained. With subsequent dilutions, the final concentration will be 1%. Prepared two solutions are mixed in a one to one (1:1) ratio. Alkaline reagent: for 0.5% NaOH; 100 mg of NaOH is weighed and dissolved in 10 mL of water[24]. For 0.1% NaOCl; 0.1105 mL of 10% NaOCl is taken and added to 10 mL of distilled water. Prepared two solutions are mixed in a one to one (1:1) ratio. We pipetted all of them into cuvettes sequentially with different pipettes and measured the activities at 630 nm wavelength. After finding a control value, we started the IC_{50} study, we found that their activities decreased by using different inhibitor concentrations, we determined that the activities decreased as the amount of inhibitor increased[25–27].

2.3 Molecular docking

In this work, molecular modeling calculations were made to compare the biochemical activities of the studied compounds and their activities were compared. As a result of these calculations, many parameters were found from the calculations. The numerical value of these parameters gives a lot of important information about the activities of molecules[28]. Calculations are made as a result of combining many modules. The first module used includes the preparation of the studied molecules for calculations. At first, optimized structures of the molecules were obtained from the Gaussian software program[29]. It was then prepared for calculations using the LigPrep module[30] using optimized structures of the molecules. In another module, studied four proteins with the protein preparation module[31] were prepared for calculations. The Glide ligand docking module was used to interact with the molecules and protein prepared later. Finally, the Qik-prop module[32] of the Schrödinger software was used to predict the effects and responses on human metabolism as working molecules as drugs. With this calculation, the absorption of the molecules into the human body, their distribution in the body, their effects and reactions in the metabolism, their excretion from the metabolism and their toxic effects are examined by ADME/T analysis (distribution, absorption, excretion, metabolism, and toxicity).

2.4 Cancer study

2.4.1 Replication of cells

In order to determine the cytotoxic activity of the compounds, human breast (MCF-7) and prostate (PC-3) cancer cell lines were obtained from the American Type Culture Collection (ATCC) and used in the study. PC-3 cell was fed with RPMI-1640 medium and MCF-7 cells were fed with DMEM medium. Cells were fed twice a week and cell flasks were incubated at 37℃ (Thermo Forma II CO_2 Incubator, USA) in a 5% CO_2 environment throughout the experimental period. Confused cells were removed with trypsin-EDTA solution and counted under the microscope after staining with 0.4% trypan blue. For experimental studies, 96-well plates were seeded with approximately 15 × 103 cells per well[33].

2.4.2 Treatment with test compounds

1-100 μM concentrations of the compounds to be tested were added to the cell seeded wells, and then the plates were incubated for 24 hours at 37℃ in a 5% CO_2 incubator. The possible effects of the applied compounds on cell viability at the end of the incubation were determined by the MTT method[34].

2.4.3 MTT method

MTT solution at a concentration of 0.5 mg/mL was prepared for the analysis of viability levels in cells after compound administration. After the application, 50 μL of MTT solution was added to each well and incubated in a CO_2 incubator for 3 hours. After incubation, the solution in the wells was withdrawn and 100 μL of DMSO was added to them. The optical density of the cells in the wells was read in an ELISA plate reader (Thermo MultiskanGo, USA) at a wavelength of 570 nm. The absorbance values obtained from the control wells were averaged and this value was evaluated as 100% cell viability. The absorbance values obtained from the compound treated wells were proportioned to the control absorbance value and the percent viability values were calculated[35, 36].

3 Results and Discussion

3.1 Enzymes results

In this study, we investigated the inhibition effects of matairesinol, pregnanolone, hamamelitannin, secoisolariciresinol, and secoisolariciresinol diglicoside compounds on HMG-CoA reductase and urease enzymes. We have obtained results for the HMG-CoA reductase enzyme at the millimolar level, and for the urease enzyme at the micromolar level. HMG-CoA reductase inhibitors also have antithrombotic properties. We obtained IC_{50} results for the HMG-CoA reductase enzyme in the range of 3.23 ± 0.31-53.44 ± 7.61 mM. Hamamelitannin and pregnanolone were considered good inhibitors for this enzyme, and their IC_{50} results were 3.23 ± 0.31 and 6.05 ± 0.84 mM, respectively. During inflammation, thrombomodulin expression decreases on the endothelial surface and tissue factor expression increases; this situation creates a tendency to thrombosis. The use of HMG-CoA reductase inhibitors increases thrombomodulin expression and decreases tissue factor synthesis and activity. In addition, antifibrinolytic factor decreases plasminogen activator inhibitor-1 levels, profibrinolytic factor increases tissue plasminogen activator expression, decreases von Willebrand factor levels and shows antiag-

Table 1 Inhibition results of some phenolic compounds on HMG-CoA reductase and urease enzymes.

NO	Compounds	HMG-CoA reductase	Urease
		IC50 (mM)	*IC50 (μM)*
1	Matairesinol	23.25 ± 4.31	0.98 ± 0.14
2	Pregnanolone	6.05 ± 0.84	1.26 ± 0.30
3	Hamamelitannin	3.23 ± 0.31	2.41 ± 0.62
4	Secoisolariciresinol	9.37 ± 1.04	14.38 ± 2.03
5	Secoisolariciresinol diglicoside	53.44 ± 7.61	10.72 ± 1.66
	Standard compound (thiourea)	–	34.27 ± 7.47

gregant effect on platelets with NO production[37]. In this way, it changes the balance of hemostasis and thrombosis from prothrombotic tendency towards fibrinolytic direction. Additionally, we obtained IC_{50} results for the urease enzyme in the range of 0.98 ± 0.14-14.38 ± 2.03 μM. Matairesinol and pregnanolone were considered good inhibitors for this enzyme, and their IC_{50} results were 0.98 ± 0.14 and 1.26 ± 0.30 μM, respectively. The diverse and important roles of urease support this enzyme to be the focus of researchers around the world in the fields of genetics, biochemistry and physiology. Strategies based on urease inhibition are considered promising tools for treating diseases caused by urease-synthesizing bacteria and reducing the loss of nitrogen from urea used as fertilizer. Therefore, it is not surprising that research on urease inhibitors has increased recently[38].

3.2 Molecular docking study

In recent studies, the most common and known method used to compare the theoretical biological activities of molecules is molecular docking. In the calculations made by this method, important information about the biological activities of molecules is obtained before experimental procedures. As a result of the interaction of molecules with proteins used in calculations, the docking score parameter is determined[39]. One of the most important factors affecting the numerical value of this parameter is the interaction between molecules and proteins[40]. Other important parameters calculated as a result of the interaction of molecules with protein are given in Table 2.

Severe acute respiratory syndrome coronavirus 2 (SARS-CoV-2) protein has many receptor points. These are spike protein, ACE 2 (angiotensin-converting enzyme 2) protein, RNA-dependent RNA polymerase (RdRp) and main protease[41]. In this study, the inhibitory activities of molecules against the RdRp protein of the SARS-CoV-2 virus were studied. The FDA (U.S. Food and Drug Administration) approved drug for the RdRp protein of the SARS-CoV-2 virus is favipiravir. This drug was used as standard in the study. Among the parameters calculated as a result of the calculations, the Glide ligand efficiency parameter, which shows the efficiency of the molecules, are the Glide hbond, Glide evdw, and Glide ecoul parameters, which show the interactions between molecules and proteins. Glide energy, Glide einternal, Glide emodel, and Glide posenum parameters provide information about the interaction pose between molecule and protein[42, 43].

The biological activities of the molecules were compared with the parameters found as a result of the molecular docking calculations. Afterward, ADME/T analysis was carried out in which calculations were made regarding the effects and responses of these drug molecules on human metabolism, the toxicity they created in human metabolism, and their excretion from human metabolism. Many parameters were found in these calculations (Table 3). Each parameter predicts a different effect and response in human metabolism. For example, the parameter QPPCaco refers to the gut-blood barrier and the parameter QPPMDCK refers to the brain-blood barrier[42]. The donorHB parameter indicates the hydrogen bond given, and the accptHB parameter indicates the number of hydrogen bonds taken[43]. Many parameters such as these are calculated. As a result of the ADME/T analysis performed for the Secoisolariciresinol diglicoside molecule, it was seen that the numerical values of many parameters were not in the desired reference range Figs. 2-5.

3.3 Cancer results

The cytotoxic effect of test compounds on human breast, and prostate cancer cell lines is shown in Figs. 6 and 7, respectively. Hamamelitannin, matairesinol and secoisolariciresinol significantly decreased MCF-7 cell viability from low doses (Fig. 6; $p<0.05$). In addition, 100 μM dose of all compounds caused significant reductions in PC-3 cell viability (Fig. 7; $p<0.05$). In general, we can say that the two tested compounds, hamamelitannin and matairesinol have cytotoxic effects in all cell types, and this effect is particularly strong in MCF-7 cells. Indeed, the search for safe, potent, and selective anticancer molecules is very important for novel drug progress in cancer research. Also, over

Table 2 Numerical values of the docking parameters of molecule against enzymes.

HMG-CoA reductase protein	Hamamelitannin (1)	Matairesinol (2)	Pregnanolone (3)	Secoisolariciresinol (4)	Secoisolariciresinol diglicoside (5)	Thiourea
Docking Score	−9.07	−5.96	−5.64	−6.39	−8.93	−4.97
Glide ligand efficiency	−0.24	−0.23	−0.25	−0.25	−0.18	−1.24
Glide hbond	0.00	0.00	−0.32	−0.65	−0.32	−0.54
Glide evdw	−40.91	−26.78	−28.77	−23.65	−42.67	−11.84
Glide ecoul	−32.43	−15.04	−4.77	−18.33	−28.06	−5.72
Glide emodel	−102.81	−55.05	−44.20	−55.40	−114.31	−24.24
Glide energy	−73.33	−41.82	−33.54	−41.98	−70.73	−17.56
Glide einternal	12.40	6.39	0.41	12.85	20.34	0.00
Glide posenum	39	373	332	353	92	191
Jack bean urease	Hamamelitannin (1)	Matairesinol (2)	Pregnanolone (3)	Secoisolariciresinol (4)	Secoisolariciresinol diglicoside (5)	Thiourea
Docking Score	−6.56	−8.82	−5.02	−5.45	−8.64	−4.64
Glide ligand efficiency	−0.19	−0.22	−0.22	−0.21	−0.17	−1.16
Glide hbond	0.00	0.00	−0.38	−0.43	−0.44	−0.32
Glide evdw	−29.29	−45.09	−13.03	−16.34	−38.39	−12.98
Glide ecoul	−24.80	−14.26	−9.72	−23.23	−27.15	−8.25
Glide emodel	−83.86	−60.74	−28.78	−49.62	−95.91	−30.26
Glide energy	−54.09	−49.35	−22.75	−39.57	−65.54	−21.23
Glide einternal	8.74	12.59	1.43	7.65	29.15	0.00
Glide posenum	385	148	73	42	24	234
SARS-CoV-2	Hamamelitannin (1)	Matairesinol (2)	Pregnanolone (3)	Secoisolariciresinol (4)	Secoisolariciresinol diglicoside (5)	Favirpiravir
Docking Score	−7.83	−8.23	−	−10.14	−	−4.94
Glide ligand efficiency	−0.23	−0.32	−	−0.39	−	−0.45
Glide hbond	−0.16	−0.01	−	−1.19	−	−0.73
Glide evdw	−20.26	−40.00	−	−34.74	−	−22.14
Glide ecoul	−23.03	−16.13	−	−24.99	−	6.34
Glide emodel	−41.33	−72.18	−	−88.78	−	−25.60
Glide energy	−43.29	−56.13	−	−59.73	−	−15.80
Glide einternal	29.00	17.93	−	12.49	−	0.00
Glide posenum	93	23	−	290	−	60
HP-5	Hamamelitannin (1)	Matairesinol (2)	Pregnanolone (3)	Secoisolariciresinol (4)	Secoisolariciresinol diglicoside (5)	Butylated hydroxyanisole
Docking Score	−5.36	−4.19	−5.05	−4.51	−6.49	−4.62
Glide ligand efficiency	−0.16	−0.16	−0.22	−0.17	−0.13	−0.36
Glide hbond	−0.16	−0.16	−0.78	0.00	0.00	−0.39
Glide evdw	−21.53	−24.14	−19.13	−21.31	−29.50	−14.22
Glide ecoul	−27.63	−10.19	−7.23	−14.35	−26.99	−5.74
Glide emodel	−62.61	−40.80	−33.40	−48.23	−76.68	−24.83
Glide energy	−49.15	−34.33	−26.37	−35.66	−56.48	−19.96
Glide einternal	6.17	4.80	1.98	5.08	27.59	0.31
Glide posenum	60	242	359	116	242	276

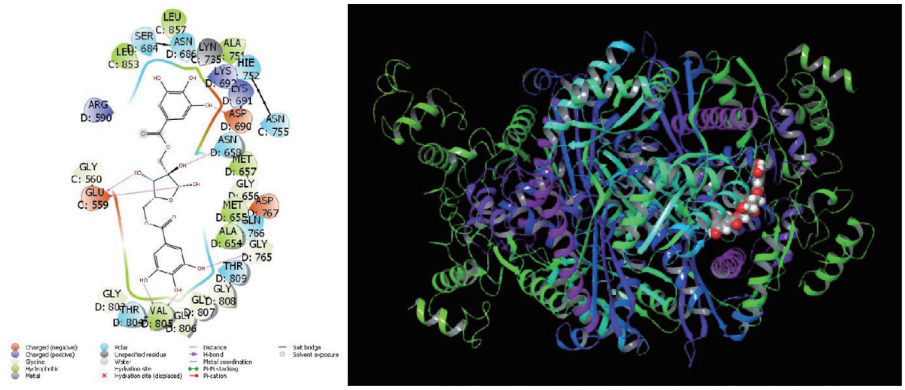

Fig. 2 Presentation interactions of secoisolariciresinol diglicoside with HP-5 protein.

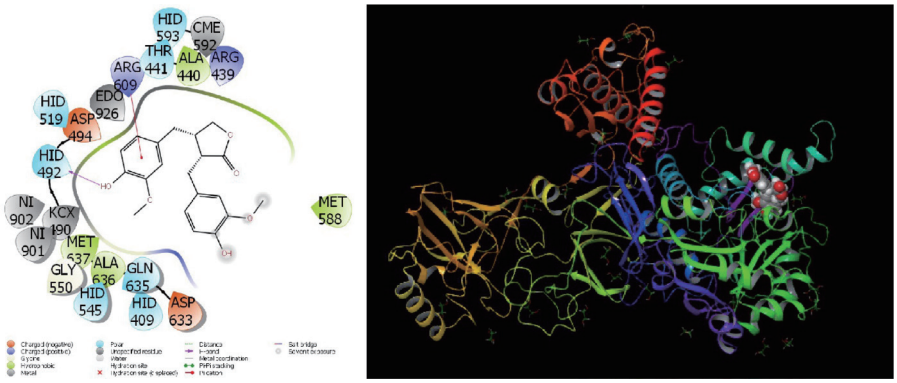

Fig. 3 Presentation interactions of hamamelitannin with HMG-CoA reductase protein.

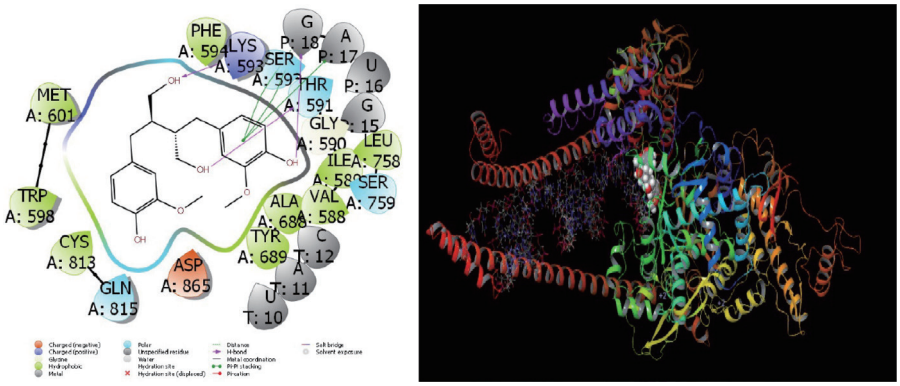

Fig. 4 Presentation interactions of matairesinol with Jack bean urease.

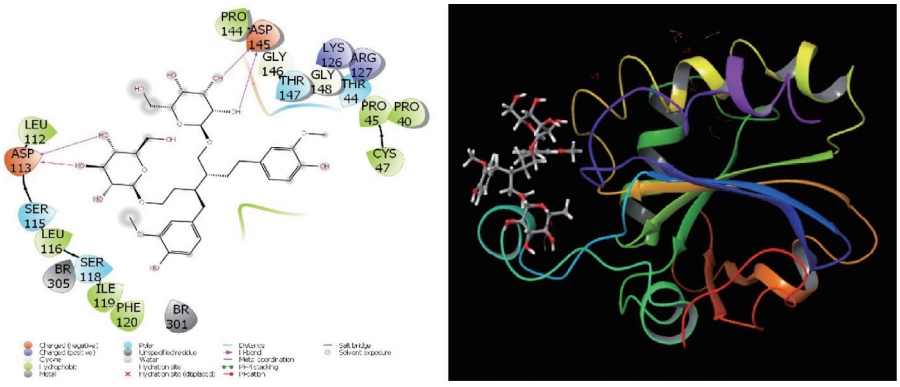

Fig. 5 Presentation interactions of secoisolariciresinol with SARS-CoV-2 virus.

Table 3 ADME/T properties of molecules.

	Matairesinol (2)	Pregnanolone (3)	Secoisolariciresinol diglicoside (5)	Secoisolariciresinol (4)	Hamamelitannin (1)	Reference Range
mol_MW	358	318	715	362	484	130-725
dipole (D)	5.8	1.7	4.4	4.5	1.5	1.0-12.5
SASA	557	564	1034	633	639	300-1000
FOSA	269	483	482	270	92	0-750
FISA	148	81	395	172	436	7-330
PISA	139	0	158	192	111	0-450
WPSA	0	0	0	0	0	0-175
volume (A^3)	1066	1057	2024	1149	1243	500-2000
donorHB	2	1	10	4	9	0-6
accptHB	6	3.7	23.4	6.4	14.35	2.0-20.0
glob (Sphere =1)	0.9	0.9	0.7	0.8	0.9	0.75-0.95
QPpolrz (A^3)	32.7	34.9	59.0	33.3	35.0	13.0-70.0
QPlogPC16	10.8	9.0	23.4	12.4	15.7	4.0-18.0
QPlogPoct	17.2	14.5	47.5	20.2	33.5	8.0-35.0
QPlogPw	10.1	6.3	37.7	13.0	29.0	4.0-45.0
QPlogPo/w	2.5	3.8	−1.3	2.4	−2.2	−2.0-6.5
QPlogS	−3.0	−4.9	−2.3	−3.2	−1.5	−6.5-0.5
CIQPlogS	−4.9	−4.1	−4.7	−4.6	−3.8	−6.5-0.5
QPlogHERG	−3.7	−3.3	−6.4	−5.1	−4.1	concern below −5
QPPCaco (nm/sec)	389	1686	2	234	1	*
QPlogBB	−1.1	−0.2	−5.8	−1.9	−4.1	−3.0-1.2
QPPMDCK (nm/sec)	178	870	1	103	0	*
QPlogKp	−3.0	−2.8	−5.6	−2.8	−7.7	cm/hr
IP (ev)	9.0	10.6	9.4	9.1	9.2	7.9-10.5
EA (eV)	0.0	−0.7	−0.1	0.1	0.6	−0.9-1.7
#metab	7	2	14	8	8	1-8
QPlogKhsa	0.1	0.7	−1.7	−0.2	−1.0	−1.5-1.5
Human Oral Absorption	3	3	1	2	1	-
Percent Human Oral Absorp.	88	100	0	83	0	**
PSA	99	46	256	103	269	7-200
RuleOfFive	0	0	3	0	2	Maximum is 4
RuleOfThree	1	0	2	1	2	Maximum is 3
Jm	0.3	0.0	0.0	0.4	0.0	-

* < 25 is poor and > 500 is great, ** < 25% is poor and > 80% is high.

60% of the anticancer drugs have their origin in one way or another from natural phenolic sources. Nature continues to be plenty of prolific source of diverse chemotypes and biologically active. Natural compounds, due to their structural diversity, provide excellent templates for the construction of novel molecules.

4 Conclusion

In this study, the inhibitory activities of molecules against the RNA-dependent RNA polymerase (RdRp) protein of the SARS-CoV-2 virus were studied. Therefore, the phenolic compounds are interesting hits for urease enzyme inhibition studies with future prospects of optimization and modification. The biological activities of the molecules were calculated with the parameters calculated in this theoretical study. Based on the molecules studied, it is hoped that it will be an important guide for designing more effective and more active new drug molecules in the future. It is thought that this study will be an important guide for future *in vitro* and *in vivo* studies. In addition, 100 μM dose of all compounds caused significant reductions in PC-3 cell viability (Fig. 7; $p < 0.05$). In general, we

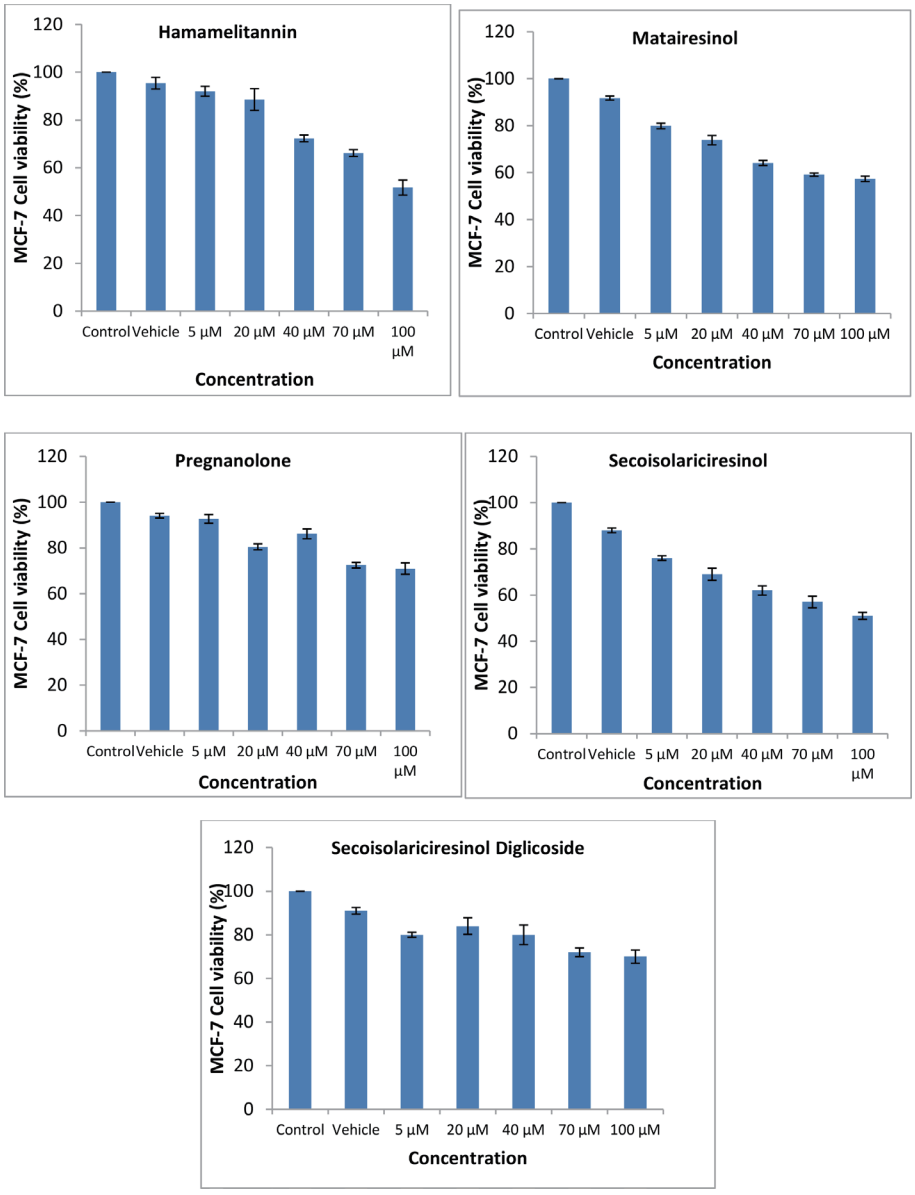

Fig. 6 Viability change (%) in human breast cancer cells 24 hours after treatment with test compounds. Data were expressed as mean ± standard deviation (n = 5). compared to the control group; compared to vehicle group (average values).

can say that the two tested compounds, hamamelitannin and matairesinol have cytotoxic effects in all cell types, and this effect is particularly strong in MCF-7 cells. In this study, hamamelitannin and pregnanolone were considered good inhibitors for HMG-CoA reductase, and their IC_{50} results were 3.23 ± 0.31 and 6.05 ± 0.84 mM, respectively. Inhibitors of this enzyme are lipid-lowering medications may use in the primary and secondary prevention of coronary heart disease.

Acknowledgement

This project was supported by Researchers Supporting Project number (RSP-2021/230) King Saud University, Riyadh, Saudi Arabia.

Conflict of Interest

There isn't any conflict of interest.

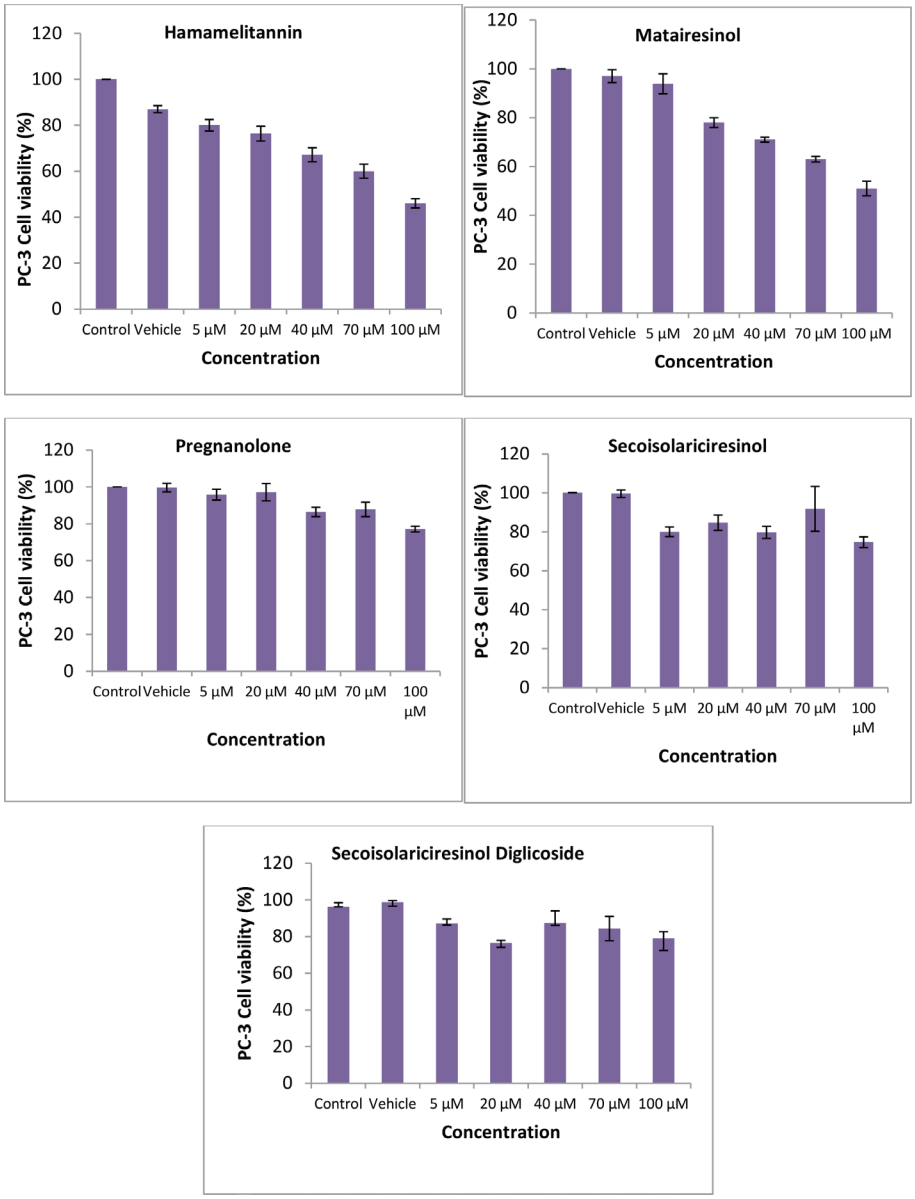

Fig. 7 Change in viability (%) in human prostate cancer cells 24 hours after treatment with test compounds. Data were expressed as mean ± standard deviation (n = 5). These values compared to vehicle group (average values).

References

1) Sun, S.Y.; Jiang, W.G.; Zhao, Y.P. Comparison of aromatic and phenolic compounds in cherry wines with different cherry cultivars by HS-SPME-GC-MS and HPLC. *Int. J. Food Sci. Technol.* **47**, 100-106 (2012).
2) Kamangerpour, A.; Ashraf-Khorassani, M.; Taylor, L.T.; McNair, H.M.; Chorida, L. Supercritical fluid chromatography of polyphenolic compounds in grape seed extract. *Chromatographia* **55**, 417-421 (2002).
3) Bourcier, T.; Libby, P. HMG CoA reductase inhibitors reduce plasminogen activator inhibitor-1 expression by human vascular smooth muscle and endothelial cells. *Arterioscler Thromb. Vasc. Biol.* **20**, 556-562 (2000).
4) Youssef, S.; Stuve, O.; Patarroyo, J.C.; Ruiz, P.J.; Radosevich, J.L. *et al.* The HMG-CoA reductase inhibitor, atorvastatin, promotes a Th2 bias and reverses paralysis in central nervous system autoimmune disease. *Nature* **420**, 78-84 (2002).
5) Rasmussen, L.M.; Hansen, P.R.; Nabipour, M.T.; Olesen, P.; Kristiansen, M.T.; Ledet, T. Diverse effects of inhibition of 3-hydroxy-3-methylglutaryl-CoA reductase on the expression of VCAM-1 and E-selectin in endothelial cells. *Biochem. J.* **360**, 363-370 (2001).
6) Laufs, U.; La Fata, V.; Plutzky, J.; Liao, J.K. Upregulation of endothelial nitric oxide synthase by HMG CoA

reductase inhibitors. *Circulation* **97**, 1129-1135 (1998).
7) Tanaka, T.; Kawase, M.; Tani, S. Urease inhibitory activity of simple-unsaturated ketones. *Life Sci.* **73**, 2985-2990 (2003).
8) Amtul, Z.; Rasheed, M.; Choudhary, M.I.; Rosanna, S.; Khan, K.M.; Atta ur Rehman. Kinetics of novel competitive inhibitors of urease enzymes by a focused library of oxadiazoles/thiadiazoles and triazoles. *Biochem. Biophys. Res. Commun.* **319**, 1053-1063 (2004).
9) Ahmad, V.U.; Hussain, J.; Hussain, H.; Jassbi, A.R.; Uullah, F. *et al.* First natural urease inhibitor from *Euphorbia decipiens*. *Chem. Pharm. Bull.* **51**, 719-723 (2003).
10) Ahmad, M.; Muhammad, N.; Ahmad, M.; Lodhi, M.A.; Jehan, N. *et al.* Urease inhibitor from *Datisca cannabina* Linn. *J. Enzyme Inhib. Med. Chem.* **23**, 386-390 (2008).
11) Moreno-Eutimio, M.A.; López-Macías, C.; Pastelin-Palacios, R. Bioinformatic analysis and identification of single-stranded RNA sequences recognized by TLR7/8 in the SARS-CoV-2, SARS-CoV, and MERS-CoV genomes. *Microbes Infect.* **22**, 226-229 (2020).
12) Shang, J.; Wan, Y.; Luo, C.; Ye, G.; Geng, Q. *et al.* Cell entry mechanisms of SARS-CoV-2. *Proc. Natl. Acad. Sci. USA* **117**, 11727-11734 (2020).
13) Koç, E.; Üngördü, A.; Candan, F. Antioxidant properties of methanolic extract of '*Veronica multifida*' and DFT and HF analyses of its the major flavonoid component. *J. Mol. Struct.* **1197**, 436-442 (2019).
14) Hillen, H.S.; Kokic, G.; Farnung, L.; Dienemann, C.; Tegunov, D.; Cramer, P. Structure of replicating SARS-CoV-2 polymerase. *Nature* **584**, 154-156 (2020).
15) Istvan, E.S.; Deisenhofer, J. Structural mechanism for statin inhibition of HMG-CoA reductase. *Science* **292**, 1160-1164 (2001).
16) Declercq, J.P.; Evrard, C.; Clippe, A.; Vander Stricht, D.; Bernard, A.; Knoops, B. Crystal structure of human peroxiredoxin 5, a novel type of mammalian peroxiredoxin at 1.5 Å resolution. *J. Mol. Biol.* **311**, 751-759 (2001).
17) Lim, J.S.; Jeon, S.; Shin, H.Y.; Kim, M.J.; Seong, Y.M. *et al.* Case of the index patient who caused tertiary transmission of COVID-19 infection in Korea: The application of lopinavir/ritonavir for the treatment of COVID-19 infected pneumonia monitored by quantitative RT-PCR. *J. Korean Med. Sci.* **35**, e79 (2020).
18) Ito, T.; Ikeda, U.; Shimpo, M.; Ohki, R.; Takahashi, M. *et al.* HMG-CoA reductase inhibitors reduce interleukin-6 synthesis in human vascular smooth muscle cells Cardiovasc. *Drugs Ther.* **16**, 121-126 (2002).
19) Inoue, I.; Goto, S.; Mizotani, K.; Awata, T.; Mastunaga, T. *et al.* Lipophilic HMG-CoA reductase inhibitor has an anti-inflammatory effect: reduction of MRNA levels for interleukin-1beta, interleukin-6, cyclooxygenase-2, and p22phox by regulation of peroxisome proliferator-activated receptor alpha (PPARalpha) in primary endothelial cells. *Life Sci.* **67**, 863-876 (2000).
20) Kita, T.; Brown, M.S.; Goldstein, J.L. Feedback regulation of 3-hydroxy-3-methylglutaryl coenzyme A reductase in livers of mice treated with mevinolin, a competitive inhibitor of the reductase. *J. Clin. Invest.* **66**, 1094-1100 (1980).
21) Mobley, H.L.; Hu, L.T.; Foxal, P.A. *Helicobacter pylori* urease: Properties and role in pathogenesis. *Scand. J. Gastroenterol. Suppl.* **187**, 39-46 (1991).
22) Sumner, J.B. The isolation and crystallization of the enzyme urease. *J. Biol. Chem.* **69**, 435-439 (1926).
23) You, Z.L.; Zhang, L.; Shi, D.H.; Wang, X.L.; Li, X.F.; Ma, Y.P. Synthesis, crystal structures and urease inhibitory activity of copper (II) complexes with Schiff bases. *Inorg. Chem. Commun.* **13**, 996-998 (2010).
24) You, Z.L.; Ni, L.L.; Shi, D.H.; Bai, S. Synthesis, structures, and urease inhibitory activities of three copper (II) and zinc (II) complexes with 2-{[2-(2-hydroxyethylamino) ethylimino] methyl} -4-nitrophenol. *Eur. J. Med. Chem.* **45**, 3196-3199 (2010).
25) Chen, W.; Li, Y.; Cui, Y.; Zhang, X.; Zhu, H.L.; Zeng, Q. Synthesis, molecular docking and biological evaluation of Schiff base transition metal complexes as potential urease inhibitors. *Eur. J. Med. Chem.* **45**, 4473-4478 (2010).
26) Amtul, Z.; Rasheed, M.; Choudhary, M.I.; Supino, R.; Khan, K.M.; Ur-Raman, A. Kinetics of novel competitive inhibitors of urease enzymes by a focused library of oxadiazoles/thiadiazoles and triazoles. *Biochem. Biophys. Res. Comm.* **319**, 1053-1063 (2004).
27) Tsuchiya, M.; Imamura, L.; Park, J.B.; Kobashi, K. *Helicobacter pylori* urease inhibition by rabeprazole, a proton pump inhibitor. *Biol. Pharm. Bull.* **18**, 1053-1056 (1995).
28) Schrodinger, L. Small-Molecule Drug Discovery Suite 2019-4 (2019).
29) Frisch, M.J.; Trucks, G.W.; Schlegel, H.B.; Scuseria, G.E.; Robb, M.A. *et al.* Gaussian 09, revision D.01. Gaussian Inc., Wallingford CT (2009).
30) Schrödinger Release 2019-4: LigPrep, Schrödinger, LLC, New York, NY (2019).
31) Schrödinger Release 2019-4: Protein Preparation Wizard; Epik, Schrödinger, LLC, New York, NY, 2016; Impact, Schrödinger, LLC, New York, NY, 2016; Prime, Schrödinger, LLC, New York, NY (2019).
32) Schrödinger Release 2020-1: QikProp, Schrödinger, LLC, New York, NY (2020).
33) Wilson, J.K.; Sargent, J.M.; Elgie, A.W.; Hill, J.G.; Taylor, C.G. A feasibility study of the MTT assay for chemosensitivity testing in ovarian malignancy. *Br. J.*

Cancer **62**, 189-194 (1990).
34) Wassermann, T.H.; Twentyman, P. Use of colorimetric microtiter (MTT) assay in determining the radiosensitivity of cells from murine solid tumors. *Int. J. Radiat. Oncol. Biol. Phys.* **15**, 699-702 (1988).
35) Van de Loosdrecht, A.A.; Nennie, E.; Ossenkoppele, G.J.; Beelen, R.H.; Langenhuijsen, M.M. Cell mediated cytotoxicity against U 937 cells by human monocytes and macrophages in a modified colorimetric MTT assay. *J. Immunol. Methods* **141**, 15-22 (1991).
36) Sargent, J.M.; Taylor, C.G. Appraisal of the MTT assay as a rapid test of chemosensitivity in acute myeloid leukaemia. *Br. J. Cancer* **60**, 206-210 (1989).
37) Yoshida, M.; Sawada, T.; Ishii, H. *et al.* HMG-CoA reductase inhibitor modulates monocyte-endothelial cell interaction under physiological flow conditions *in vitro*: Involvement of Rho GTPase-dependent mechanism. *Arterioscler. Thromb. Vasc. Biol.* **21**, 1165-1171 (2001).
38) Kuhler, T.C.; Fryklund, J.; Bergman, N.A.; Weilitz, J.; Lee, A.; Larsson, H. Structure-activity relationship of omeprazole and analogs as *Helicobacter pylori* urease inhibitors. *J. Med. Chem.* **38**, 4906-4916 (1995).
39) Jin, Z.; Du, X.; Xu, Y.; Deng, Y.; Liu, M. *et al.* Structure of Mpro from COVID-19 virus and discovery of its inhibitors. *Nature* **582**, 289-293 (2020).
40) Kai, K.; Cohen, J. Race to find COVID-19 treatments accelerates. *Science* **367**, 1412-1413 (2014).
41) Ren, J.L.; Zhang, A.H.; Wang, X.J. Corrigendum to 'Traditional Chinese medicine for COVID-19 treatment'. *Pharmacol. Res.* **155**, 104743 (2020).
42) Chang, Y.; Tung, Y.; Lee, K.; Chen, T.; Hsiao, Y. *et al.* Potential therapeutic agents for COVID-19 based on the analysis of protease and RNA polymerase docking. *Virol. J.* (2020).
43) Gautret, P.; Lagier, J.-C.; Parola, P.; Hoang, V.T.; Meddeb, L. *et al.* Hydroxychloroquine and azithromycin as a treatment of COVID-19: results of an open-label nonrandomized clinical trial. *Int. J. Antimicrob. Agents* **56**, 105949 (2020).